PRAMANA
— journal of
physics

Vol. 63, No. 5
November 2004
pp. 1053–1062

Scaling of cross-sections for asymmetric $(e, 3e)$ process on helium-like ions by fast electrons

M K SRIVASTAVA
Institute Instrumentation Centre, Indian Institute of Technology,
Roorkee 247 667, India
E-mail: mksrific@iitr.ernet.in

MS received 26 December 2003; revised 30 April 2004; accepted 15 June 2004

Abstract. An approximate simple scaling law is obtained for asymmetric $(e, 3e)$ process on helium-like ions for double ionization by fast electrons. It is based on the equation $(Z'^3/\pi)\exp[-Z'(r_1 + r_2)]$, $Z' = Z - (5/16)$ for ground state wave function of helium-like ions and Z'^2 scaling of energies. The scaling law is found to work very well if the lower energy electron is ejected along the momentum transfer direction and the other one is ejected in the opposite direction. It also works quite well if this electron is ejected within about 90° of the momentum transfer direction with the other electron going in the opposite direction. The scaling law becomes increasingly accurate as the target nuclear charge and the energy increase.

Keywords. $(e, 3e)$ process; five-fold differential cross-section; scaling; helium isoelectronic ions.

PACS No. 34.80.Dp

1. Introduction

The theoretical description of the $(e, 3e)$ process is a difficult task because the motion of the four charged particles in the final state remains correlated even at large separations due to the infinite range of the Coulomb force. The helium atom being the simplest target for this study, is the easiest to handle. The residual ion is simply the bare nucleus and the complications due to the residual core are absent. Several calculations of the five-fold differential cross-section (FDCS) for the $(e, 3e)$ process on helium in different kinematical arrangements and at different initial energies have been performed and the results have been compared with experiment [1–9]. The agreement is found to be reasonably good. However, experiments with helium-like systems $(Z > 2)$ are not easily performed. The preparation and experimental control of the target and the intensity related problems make the measurements extremely difficult. The scaling laws of differential cross-section offer a workable and convenient way to study the general behaviour (angular

Table 1.

	Hartree–Fock wave function			Choice (1)	
Z	Exponent of the dominant term	Coefficient of the dominant term	Binding energy	Error in the exponent	Binding energy
2	1.453	0.830	0.2862(+1)	16.14%	0.2848(+1)
10	9.455	0.970	0.9386(+2)	2.46%	0.9385(+2)
20	19.453	0.985	0.3876(+3)	1.21%	0.3876(+3)
30	29.457	0.990	0.8814(+3)	0.78%	0.8813(+3)
36	35.449	0.997	0.1274(+4)	0.67%	0.1274(+4)

distribution and magnitude) of the cross-section and to provide further insight into the process. The scaling of triple differential cross-section (TDCS) for the electron impact single ionization of hydrogenic targets has been tried earlier by Berakdar *et al* [10] and Spivack *et al* [11] and more recently by Stia *et al* [12]. The problem here is relatively simpler. The target ground state wave function is exactly known and has a definite Z dependence. An exact scaling is possible for the first-order Born approximation irrespective of kinematical and geometric conditions. It is also valid in the Coulomb–Born approximation for high enough Z and incident energies. The scaled behaviour of the differential cross-section for the ionization of hydrogen by the impact of fast electrons, positrons, protons and antiprotons has also been recently analysed by Jones and Madison [13]. They have studied dependence of TDCS on the projectile charge and mass.

An exact scaling in the case of $(e, 3e)$ process on helium-like targets is not possible even in the first-order Born approximation. Besides a more complex final state, the target initial state wave function is not exactly known. The one-parameter variational wave function of helium ground state

$$\varphi_i(\vec{r}_1, \vec{r}_2) = \frac{Z'^3}{\pi} \mathrm{e}^{-Z'(r_1+r_2)}, \tag{1}$$

where $Z' = Z - 5/16$, $Z = 2$, is known to be quite poor. However, as Z increases, this wave function gives an improved description of the ground state and the binding energy. Table 1 gives the exponent and coefficient of the dominant term in the wave function and the binding energy of helium isoelectronic positive ions up to $Z = 36$ corresponding to Hartree–Fock wave functions of Clementi and Roetti [14]. They are compared with the values obtained by using the choice (1).

It is observed that as Z increases, choice (1) for the target ground state wave function becomes quite reasonable. We have used this choice. It lacks in radial and angular e–e correlation and may not be very good but has the advantage of having a simple and explicit Z dependence, which is crucial to any scaling law.

2. Theory

The FDCS for the process

$$e + (Z + e + e) \rightarrow e + Z + e + e$$

in which a fast electron with energy E_i (momentum $\vec{k}_i$) is scattered with energy E_a (momentum $\vec{k}_a$) in a direction ϑ_a, φ_a by a helium isoelectronic ion of nuclear charge Z and two target electrons are ejected with energies E_b and E_c (momenta $\vec{k}_b$, $\vec{k}_c$) in directions ϑ_b, φ_b and ϑ_c, φ_c respectively, is given by

$$\frac{\mathrm{d}^5\sigma}{\mathrm{d}E_b \mathrm{d}E_c \mathrm{d}\Omega_a \mathrm{d}\Omega_b \mathrm{d}\Omega_c} = (2\pi)^4 \frac{k_a k_b k_c}{k_i} |T_{fi}|^2. \tag{2}$$

The energy conservation requires $E_i - I = E_a + E_b + E_c$. Here I is the binding energy of the target. The scattering matrix element T_{fi} assuming shake-off is given by

$$T_{fi} = \langle \Psi_f^- | V_i | \Psi_i \rangle, \tag{3}$$

where

$$\Psi_i(\vec{r}_0, \vec{r}_1, \vec{r}_2) = F_c \langle \vec{k}_i, \vec{r}_0 \rangle \phi_i \langle \vec{r}_1, \vec{r}_2 \rangle, \tag{4}$$

$$F_c(\vec{k}_i, \vec{r}_0) = (2\pi)^{-3/2} \exp(-\pi\alpha_i/2)\Gamma(1 + i\alpha_i) \exp(i\vec{k}_i \cdot \vec{r}_0) \times {}_1\vec{F}_1(-\vec{i}\alpha_i; 1; i(k_i r_0 - \vec{k}_i \cdot \vec{r}_0)), \tag{5}$$

$$\alpha_i = -(Z - 2)/k_i, \tag{6}$$

$$V_i = \frac{1}{r_{01}} + \frac{1}{r_{02}} - \frac{2}{r_0}, \tag{7}$$

$$r_{0j} = |\vec{r}_0 - \vec{r}_j|.$$

The final state wave function is approximated as

$$\Psi_f^- = (2\pi)^{-9/2} \exp[i(\vec{k}_a \cdot \vec{r}_0 + \vec{k}_b \cdot \vec{r}_1 + \vec{k}_c \cdot \vec{r}_2)] C(\alpha_a, \vec{k}_a, \vec{r}_0) \times C(\alpha_b, \vec{k}_b, \vec{r}_1) C(\alpha_c, \vec{k}_c, \vec{r}_2) C(\alpha_{bc}, \vec{k}_{bc}, \vec{r}_{12}), \tag{8}$$

where

$$C(\alpha, \vec{k}, \vec{r}) = \Gamma(1 - i\alpha) \mathrm{e}^{-\pi\alpha/2} {}_1F_1(i\alpha; 1; -i(kr + \vec{k} \cdot \vec{r})) \tag{9}$$

and the Sommerfeld parameters α_a, α_b, α_c and α_{bc} are defined as [15]

$$\alpha_a = -(Z - 2)/k_a, \tag{10}$$

$$\alpha_b = -\frac{1}{k_b} \left[Z \left(1 + \frac{k_b}{2k_a} \right) - \frac{k_b}{|\vec{k}_a - \vec{k}_b|} \right], \tag{11}$$

$$\alpha_c = -\frac{1}{k_c} \left[Z \left(1 + \frac{k_c}{2k_a} \right) - \frac{k_c}{|\vec{k}_a - \vec{k}_c|} \right], \tag{12}$$

$$\alpha_{bc} = \frac{1}{2k_{bc}}. \tag{13}$$

Finally the T-matrix element may be written as

$$\begin{aligned} T_{fi} = (2\pi)^{-6} N \left(\frac{Z'^3}{\pi}\right) \\ \times \int \mathrm{d}\vec{r}_0 \mathrm{d}\vec{r}_1 \mathrm{d}\vec{r}_2 \exp[i(\vec{k}_i \cdot \vec{r}_0 - \vec{k}_a \cdot \vec{r}_0 - \vec{k}_b \cdot \vec{r}_1 - \vec{k}_c \cdot \vec{r}_2)] \\ \times {}_1F_1(-i\alpha_i; 1; i(k_i r_0 - \vec{k}_i \cdot \vec{r}_0)) {}_1F_1(-i\alpha_a; 1; i(k_a r_0 + \vec{k}_a \cdot \vec{r}_0)) \\ \times {}_1F_1(-i\alpha_b; 1; i(k_b r_1 - \vec{k}_b \cdot \vec{r}_1)) {}_1F_1(-i\alpha_c; 1; i(k_c r_2 + \vec{k}_c \cdot \vec{r}_2)) \\ \times {}_1F_1(-i\alpha_{bc}; 1; i(k_{bc} r_{12} + \vec{k}_{bc} \cdot \vec{r}_{12})) \\ \times \left(\frac{1}{r_{01}} + \frac{1}{r_{02}} - \frac{2}{r_0}\right) \mathrm{e}^{-Z'(r_1+r_2)}, \end{aligned} \tag{14}$$

where

$$\begin{aligned} N = \Gamma(1+i\alpha_i)\Gamma(1+i\alpha_a)\Gamma(1+i\alpha_b)\Gamma(1+i\alpha_c)\Gamma(1+i\alpha_{bc}) \\ \times \exp\left[-\frac{1}{2}\pi(\alpha_i + \alpha_a + \alpha_b + \alpha_c + \alpha_{bc})\right]. \end{aligned}$$

3. Scaling procedure

We now consider the scaling. It is valid when the energies and the nuclear charge are sufficiently high. Let the incident energy be scaled as

$$E_i^{(Z_2)} = \left(\frac{Z_2'}{Z_1'}\right)^2 E_i^{(Z_1)}, \tag{15}$$

which is equivalent to the following scaling in the initial momentum

$$k_i^{(Z_z)} = \left(\frac{Z_2'}{Z_1'}\right) k_i^{(Z_1)}. \tag{16}$$

From the energy conservation and the value of the binding energy $I = Z'^2$,

$$k_i^2 - Z'^2 = k_a^2 + k_b^2 + k_c^2, \tag{17}$$

we find that k_a, k_b and k_c scale in the same way as k_i. With these scalings, the Sommerfeld parameter α_i in the entrance channel varies as

$$\alpha_i^{(Z_2)} = -\frac{Z_2 - 2}{k_i^{(Z_2)}} = -\frac{Z_2 - 2}{Z_1 - 2} \cdot \frac{Z_1'}{Z_2'} \cdot \frac{Z_1 - 2}{k_i^{(Z_1)}} = \frac{Z_2 - 2}{Z_1 - 2} \cdot \frac{Z_1'}{Z_2'} \alpha_i^{(Z_1)}. \tag{18}$$

However, at a fixed incident energy, the scaling of α_i improves as Z increases, and

$$\alpha_i^{(Z_2)} \cong \alpha_i^{(Z_1)}. \tag{19}$$

Similar is the case with α_a. Let us now consider the variation of α_b and α_c. The definitions (11) and (12) lead to

$$\alpha_b^{(Z_2)} \cong \alpha_b^{(Z_1)}, \quad \alpha_c^{(Z_2)} \cong \alpha_c^{(Z_1)} \tag{20}$$

as Z increases if $\vec{k}_b, \vec{k}_c \ll \vec{k}_a$. The parameter α_{bc} does not scale. However, if $\vec{k}_{bc} \gg 1$ (asymmetric kinematics), α_{bc} vanishes and the corresponding hypergeometric function and the Coulomb phase factor tend to unity. This feature is also true for $\alpha_i(\alpha_a)$ at large enough $\vec{k}_i(\vec{k}_a)$ for all values of Z.

The coordinates $\vec{r}_i$ $(i = 0, 1, 2)$ may be scaled in the following natural way:

$$r_i^{(Z_z)} = \left(\frac{Z_1'}{Z_2'}\right) r_i^{(Z_1)}. \tag{21}$$

The coordinates $\vec{r}_{01}, \vec{r}_{02}, \vec{r}_{12}$ transform in the same way as $\vec{r}_0, \vec{r}_1$ or $\vec{r}_2$. The volume element shall scale as

$$(\mathrm{d}\vec{r}_0\, \mathrm{d}\vec{r}_1\, \mathrm{d}\vec{r}_2)^{(Z_2)} = \left(\frac{Z_1'}{Z_2'}\right)^9 (\mathrm{d}\vec{r}_0\, \mathrm{d}\vec{r}_1\, \mathrm{d}\vec{r}_2)^{(Z_1)}. \tag{22}$$

Finally the matrix element T_{fi} scales as

$$\begin{aligned} &T_{fi}^{(Z_2)}(E_i^{(Z_2)}, E_b^{(Z_2)}, E_c^{(Z_2)}) \\ &= \left(\frac{Z_1'}{Z_2'}\right)^5 T_{fi}^{(Z_1)}\left(\left(\frac{Z_1'}{Z_2'}\right)^2 E_i^{(Z_2)}, \left(\frac{Z_1'}{Z_2'}\right)^2 E_b^{(Z_2)}, \left(\frac{Z_1'}{Z_2'}\right)^2 E_c^{(Z_2)}\right) \end{aligned} \tag{23}$$

and the FDCS as

$$\begin{aligned} &\frac{\mathrm{d}^5\sigma(Z_2)}{\mathrm{d}E_b \mathrm{d}E_c \mathrm{d}\Omega_a \mathrm{d}\Omega_b \mathrm{d}\Omega_c}(E_i^{(Z_2)}, E_b^{(Z_2)}, E_c^{(Z_2)}) \\ &= \left(\frac{Z_1'}{Z_2'}\right)^8 \frac{\mathrm{d}^5\sigma(Z_1)}{\mathrm{d}E_b \mathrm{d}E_c \mathrm{d}\Omega_a \mathrm{d}\Omega_b \mathrm{d}\Omega_c} \\ &\times \left(\left(\frac{Z_1'}{Z_2'}\right)^2 E_i^{(Z_2)},\ \left(\frac{Z_1'}{Z_2'}\right)^2 E_b^{(Z_2)},\ \left(\frac{Z_1'}{Z_2'}\right)^2 E_c^{(Z_2)}\right). \end{aligned} \tag{24}$$

If we limit the present study to the kinematics commonly used in which the incident and the scattered electrons have high energies and the ejected electrons relatively low energies, $\alpha_i \cong 0$, $\alpha_a \cong 0$. The parameters α_b and α_c scale approximately but this improves as Z increases. The parameter α_{bc} does not scale but will not affect much if $k_{bc} \gg 1$, $E_b \neq E_c$.

4. Results

In figure 1 we present scaled FDCS calculated at incident energy $E_i = Z'^2 * 1000\,\mathrm{eV}$, scattering angle $\vartheta_a = 0.5°$, ejected electron energies $E_b = Z'^2 * 20$ eV, $E_c = Z'^2 *$

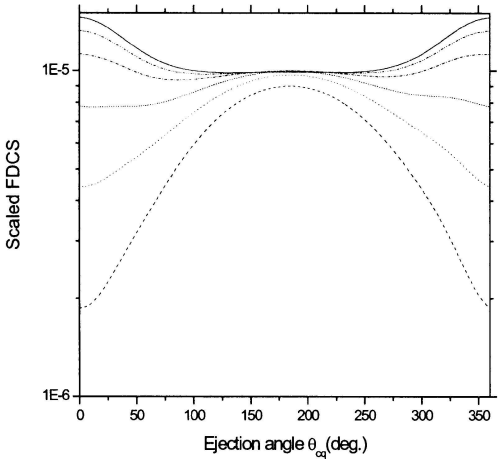

Figure 1. FDCS at incident energy $E_i = Z'^2 * 1000$ eV, scattering angle $\vartheta_a = 0.5^\circ$, ejected electron energies $E_b = Z'^2 * 20$ eV, $E_c = Z'^2 * 80$ eV. Electron b is ejected along the momentum transfer direction. The angle of ejection ϑ_{cq} of the other electron with respect to momentum transfer direction is varied. Results: $Z = 2$ (– –), $Z = 3$ (- - -), $Z = 5$ ($\cdots$), $Z = 10$ (–·–·–), $Z = 20$ (–··–··–), $Z = 50$ (—).

80 eV and ejection angle ϑ_b, φ_b along the momentum transfer direction $\vartheta_q = 6.5^\circ$, $\varphi_q = 180^\circ$ for target $Z = 2, 3, 5, 10, 20$ and 50. The ejection angle ϑ_c is varied. At these values of E_i and E_a we have taken the parameters α_i and α_a to be equal to 0. The approach of the results to the asymptotic value (for large Z) is quite clear as Z changes from 2 to 50. It is slower for lower values of Z. The cross-sections for $Z = 5$–50 at $\vartheta_{cq} = 180^\circ$ (opposite to the momentum transfer direction) almost coincide indicating perfect scaling. Here the results are least dependent on the Sommerfeld parameter α_{bc} which does not scale. Away from this value of ϑ_{cq}, the results show a gradual change with Z. The change is maximum at $\vartheta_{cq} = 0$ where α_{bc} is largest and the scaling is poor.

In figure 2 we show results at $E_i = Z'^2 * 1000$ eV, $\vartheta_a = 0.5^\circ$ but for $E_b = E_c = Z'^2 * 20$ eV and fixed $|\vartheta_b - \vartheta_c| = 180^\circ$ for target $Z = 2$, 5, 10, 20 and 50. The angle ϑ_b (or ϑ_c) is varied with respect to the momentum transfer direction. The FDCS show quite a structure with maxima at 0°, 90°, 180°, 270° and 360°, and minima at 60°, 120°, 240° and 300° for all values of Z. The angular variation is naturally symmetric about $\vartheta_{bq} = 180^\circ$. The maxima at 0° and 180° are larger. The results for different Z do not coincide at any value of ϑ_{bq} and show a quantitative variation by a factor of 1/2 as Z changes by a factor of 25. The scaling in this case does not appear to be very good perhaps due to the fact that $E_b = E_c$.

Figure 3 shows results at $E_i = Z'^2 * 1000$ eV, $|\vartheta_b - \vartheta_c| = 180^\circ$ but for $E_b = Z'^2 *$ 40 eV, $E_c = Z'^2 * 60$ eV. The angle ϑ_b is varied over the range -90° to 90° with respect to momentum transfer direction. The scaling is found to improve quite a bit. In figure 4 we take E_b and E_c still more dissimilar, $E_b = Z'^2 * 20$ eV, $E_c = Z'^2 *$ 80 eV. The scaling is now very good with the results for different Z (except $Z = 2$) almost coinciding.

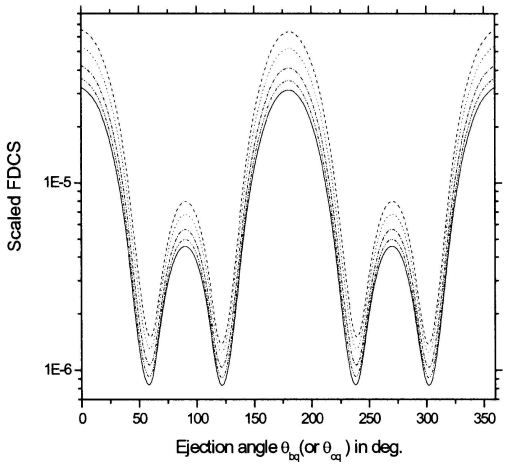

Figure 2. FDCS at $E_i = Z'^2 * 1000$ eV, $\vartheta_a = 0.5°$, $E_b = E_c = Z'^2 * 20$ eV. The electrons b and c are ejected in opposite directions, $|\vartheta_b - \vartheta_c| = 180°$. The angle ϑ_{bq} (and consequently ϑ_{cq}) is varied. Results: $Z = 2$ (– –), $Z = 5$ $(\cdots)$, $Z = 10$ $(-\cdot-\cdot-)$, $Z = 20$ $(-\cdot\cdot-\cdot\cdot-)$, $Z = 50$ (—).

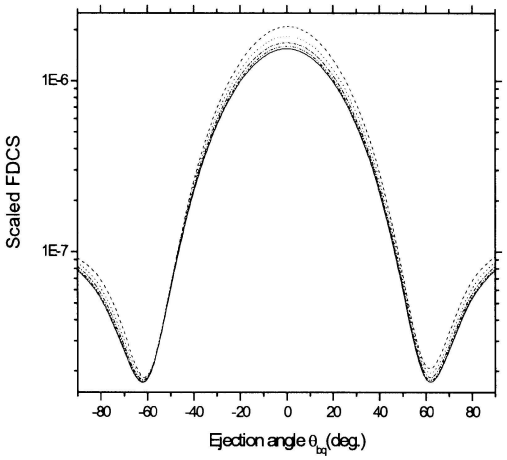

Figure 3. FDCS at $E_i = Z'^2 * 1000$ eV, $\vartheta_a = 0.5°$, $E_b = Z'^2 * 40$ eV, $E_c = Z'^2 * 60$ eV, $|\vartheta_b - \vartheta_c| = 180°$. The angle ϑ_b is varied from $-90°$ to $90°$ with respect to momentum transfer direction. Results: $Z = 2$ (– –), $Z = 5$ $(\cdots)$, $Z = 10$ $(-\cdot-\cdot-)$, $Z = 20$ $(-\cdot\cdot-\cdot\cdot-)$, $Z = 50$ (—).

We now show our results again at $E_i = Z'^2 * 1000$ eV, $\vartheta_a = 0.5°$ for fixed ϑ_c along the direction $\vartheta_q = 7.5°$ of momentum transfer and fixed ϑ_b at 180° to it. The energies E_b and E_c are varied with $E_b + E_c = Z'^2 * 80$ eV (figure 5), $Z'^2 * 100$ eV (figure 6) and $Z'^2 * 120$ eV (figure 7). The slopes of FDCS with respect to E_b/Z'^2 show slight increase with target Z in all the three cases and the results (except $Z = 2$) cross each other at $E_b/Z'^2 = 67$ eV, 80 eV and 94 eV respectively. The

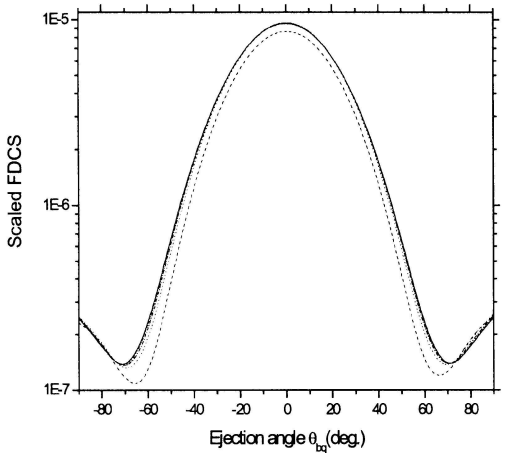

Figure 4. Same as figure 3 but $E_b = Z'^2 * 20$ eV and $E_c = Z'^2 * 80$ eV.

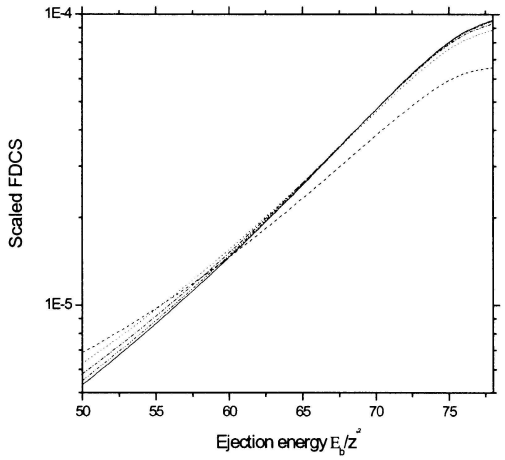

Figure 5. FDCS at $E_i = Z'^2 * 1000$ eV, $\vartheta_a = 0.5^\circ$ for ϑ_c (and ϑ_b) fixed along (opposite to) the momentum transfer direction. The energies E_b and E_c are varied with $E_b + E_c$ fixed at $Z'^2 * 80$ eV. Results: $Z = 2$ (– –), $Z = 5$ ($\cdots$), $Z = 10$ (–·–·–), $Z = 20$ (–··–··–), $Z = 50$ (—).

scaling appears to be quite reasonable in this geometry. The spread in the results at higher values of E_b in figures 5–7 is much less than at lower values. This again indicates a better scaling when the energies are dissimilar and the electron ejected along ϑ_q is of lower energy.

The change in the results with Z is expectedly largest at lower values of Z in all kinematical conditions considered here. This change becomes smaller and smaller as Z increases indicating increasing accuracy of the present scaling law.

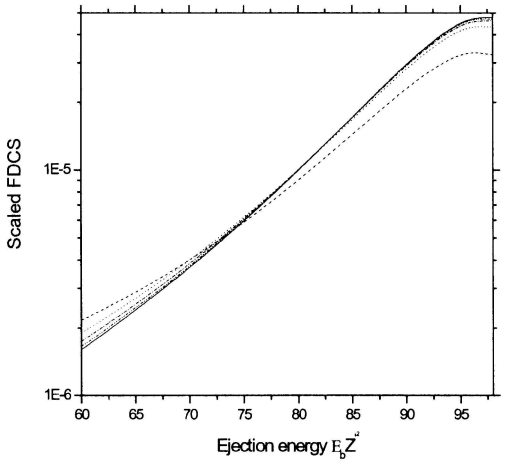

Figure 6. Same as figure 5 but for $E_b + E_c = Z'^2 * 100$ eV.

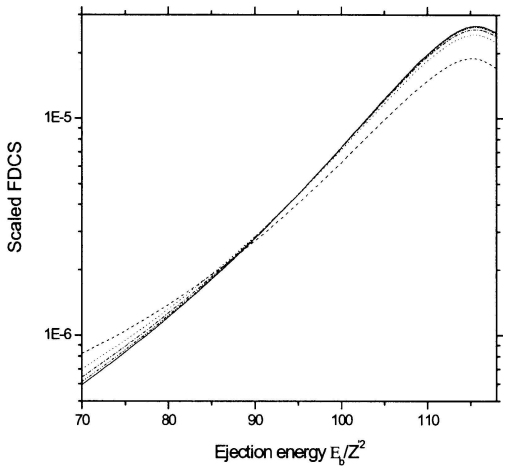

Figure 7. Same as figure 5 but for $E_b + E_c = Z'^2 * 120$ eV.

5. Conclusions

It is found that in the kinematical arrangement where the angle ϑ_{bc} between the ejected electrons (electron b along ϑ_q, and ϑ_c varying) varies, the scaling is poor in general. This is expected since the Sommerfeld parameter α_{bc} does not scale. However, when the higher energy electron c is ejected along $\vartheta_q + 180°$, the results come very close to each other indicating good scaling.

In the arrangements where ϑ_{bc} is kept fixed preferably at 180° so that α_{bc} is the smallest, the results for all values of Z considered here show the same general structure, but the scaling is not good if $E_b = E_c$. For example, the results in figure 2 change by a factor of about half when Z changes from 2 to 50. However,

if $E_b \neq E_c$, the scaling is very good over the range $-90^\circ \leq \vartheta_b \leq 90^\circ$ with respect to momentum transfer direction.

In the cases where the ejection direction of the electrons b and c is kept fixed along the momentum transfer direction and opposite to it respectively and the energies E_b and E_c are varied for fixed $E_b + E_c$, the results are very close to each other, and the scaling is found to be quite reasonable.

In short, the scaling proposed here has a limited range of applicability. It works very well if the electron ejected with lower energy is ejected along the momentum transfer direction and the other electron having higher energy is ejected in the opposite direction. It also works quite well if the direction of the lower energy electron is varied in the range $-90^\circ \leq \vartheta_b \leq 90^\circ$ with respect to momentum transfer direction with $|\vartheta_b - \vartheta_c| = 180^\circ$. The usefulness of the present results is naturally limited to kinematical arrangements where the target e–e correlations do not affect the results very much.

Acknowledgement

This work was supported by the Council of Scientific and Industrial Research, Government of India, under project No. 21(0497).

References

[1] P Lamy, B Joulakian, C Dal Cappello and A Lahmam-Bennani, *J. Phys.* **29**, 2315 (1996)
[2] M K Srivastava, S Gupta and C Dal Cappello, *Phys. Rev.* **A53**, 4104 (1996)
[3] C Dal Cappello, R E Mkhanter and P A Hervieux, *Phys. Rev.* **A57**, 693 (1998)
[4] R E Mkhanter and C Dal Cappello, *J. Phys.* **B31**, 301 (1998)
[5] I Taouil, A Lahmam-Bennani, A Duguet and L Avaldi, *Phys. Rev. Lett.* **81**, 4600 (1998)
[6] A Lahmam-Bennani, I Taouil, A Duguet, M Lecas, L Avaldi and J Berakdar, *Phys. Rev.* **A59**, 3548 (1999)
[7] A Kheifets, I Bray, A Lahmam-Bennani, A Duguet and I Taouil, *J. Phys.* **B32**, 5047 (1999)
[8] M Grin, C Dal Cappello, R E Mkhanter and J Rasch, *J. Phys.* **B33**, 131 (2000)
[9] M K Srivastava and K Muktavat, *Pramana – J. Phys.* **58**, 647 (2002)
[10] J Berakdar, J S Briggs and H Klar, *J. Phys.* **B26**, 285 (1993)
[11] R O Spivack, J Rasch, C T Whelan, R J Allan and H R J Walters, *J. Phys.* **B31**, 845 (1998)
[12] C R Stia, O A Fojon and R D Rivarola, *J. Phys.* **B33**, 1211 (2000)
[13] S Jones and D H Madison, *Phys. Rev.* **A65**, 052727-1 (2002)
[14] E Clementi and E Roetti, *At. Data Nucl. Data Tables* **14**, 177 (1974)
[15] P Defrance, T M Kereselidze, Z S Machavariani and J V Mabonia, *J. Phys.* **B32**, 2227 (1999)